Environmental Advances 24 (2026) 100714

Contents lists available at ScienceDirect

Environmental Advances

journal homepage: www.sciencedirect.com/journal/environmental-advances

Ecological risk associated with potentially toxic elements in agricultural soils across coastal and highland valleys

Wendy E. Pérez [a], Dennis Ccopi [b,*], Ricardo Flores-Marquez [a], Carlos Carbajal [a], Samuel Pizarro [b]

[a] Dirección de Servicios Estratégicos Agrarios, Instituto Nacional de Innovación Agraria (INIA), Lima, Peru
[b] Estación Experimental Agraria Santa Ana, Dirección de Servicios Estratégicos Agrarios, Instituto Nacional de Innovación Agraria (INIA), Carretera Saños Grande – Hualahoyo Km 8 Santa Ana, Huancayo, Junín 12006, Peru

ARTICLE INFO

Keywords:
Potentially toxic elements
Soil contamination
Ecological risk assessment
Spatial variability
Agroecosystems
Andean valleys
Environmental gradients
Variance partitioning

ABSTRACT

Soil elemental composition in heterogeneous agroecosystems is shaped by interacting environmental and anthropogenic controls. This study evaluated the spatial variability of potentially toxic elements (PTEs: Cu, Cr, Fe, Mn, Mo, Ni, Pb, V, Zn, As, and Cd) across coastal (Chancay and Pativilca) and highland (Mantaro and Tarma) agricultural valleys of Peru. A stratified sampling design was combined with multivariate analyses (PCA, PERMANOVA, PERMDISP, and variance partitioning) and ecological risk assessment using integrated indices (PLI, mCd, SRI, and Nemerow index). The first two principal components explained 50.2 % of total variance (PC1 = 36.8 %; PC2 = 13.4 %), reflecting distinct soil–geochemical and climatic–spatial gradients. The Valley × Zone interaction significantly structured elemental composition ($R^2 = 0.049$, $p = 0.011$), whereas crop type showed no significant effect ($p = 0.838$). Variance partitioning indicated that soil physicochemical, climatic, and spatial/topographic predictors jointly explained 60 % of total variation (adjusted $R^2 = 0.597$), with the three-way shared fraction accounting for 28 %, highlighting strong coupling among pedogenic, climatic, and topographic drivers. Ecological risk indices revealed clear spatial differentiation between systems. Highland valleys exhibited greater contamination intensity, spatial heterogeneity, and more frequent high-risk categories according to PLI, mCd, and SRI. In contrast Coastal valleys showed more homogeneous and diffuse accumulation patterns associated with long-term agricultural intensification. These findings underscore the need for regionally adapted soil monitoring frameworks that incorporate environmental gradients in the assessment and management of PTE-related ecological risk in agricultural landscapes.

1. Introduction

Soil is a complex ecosystem that supports a wide diversity of organisms and plays an essential role in food production. Its composition is influenced by both geogenic and anthropogenic factors, and an inherent characteristic of this system is its heterogeneity, which decisively conditions soil fertility and manifests as marked spatial and temporal variability in properties regulated by the interaction between environmental gradients and pedogenic processes (Minnikova et al., 2025; Pučko et al., 2024; Schneider et al., 2026). In this context, soil elemental composition constitutes a key indicator of baseline edaphic conditions and environmental quality, reflecting the combined influence of climatic conditions, mineralogical processes, water dynamics, and anthropogenic pressures across the landscape (Minnikova et al., 2025; Zeng et al., 2026).

Among the environmental factors governing this spatial heterogeneity, altitudinal gradients exert a particularly strong influence. Elevation modulates temperature, precipitation, and the processes of erosion, transport, and deposition of soil materials, thereby shaping soil physical and chemical properties and reinforcing the heterogeneity of edaphic systems across the landscape (Mangral et al., 2023; Sun et al., 2025; Vereecken et al., 2016; Zhou et al., 2023). These variations are reflected in differences in both soil characteristics and cropping systems linked to local environmental conditions. Superimposed on this topographic control, parent material stands out as one of the most influential determinants of soil genesis and geochemical composition. Geological formations condition the diversity of soil physical, chemical, and mineralogical properties, thereby determining its edaphic state (Rahayu

* Corresponding author.
E-mail address: dennisccopit@gmail.com (D. Ccopi).

https://doi.org/10.1016/j.envadv.2026.100714
Received 3 March 2026; Received in revised form 21 April 2026; Accepted 6 May 2026
Available online 6 May 2026

et al., 2023; Wilson, 2019) and directly influencing the availability and spatial distribution of macro- and micronutrients. While macronutrients are primarily associated with plant growth and development, micronutrients participate in essential metabolic and biogeochemical processes (Peng et al., 2022; Venkateswarlu et al., 2025; Xing et al., 2025). Elements such as Ca, Mg, K, Fe, Mn, and Zn are integral components of soil elemental composition whose dynamics are strongly controlled by parent material and environmental gradients.

Beyond essential nutrients, trace elements and potentially toxic elements (PTEs) represent a critical dimension of soil geochemistry. These elements occur naturally in soils, with concentrations varying according to location, parent material, and environmental conditions (Binde et al., 2025; Bauer et al., 2026). However, anthropogenic activities, including agriculture, transportation, and industrial and mining processes, can substantially increase their concentrations (Bautista-Cruz et al., 2011; Chand et al., 2024; Wu et al., 2021). Because of their persistence, mobility, bioaccumulation capacity, and potential for biomagnification, PTEs pose significant risks to ecosystems and human health (Binde et al., 2025). Soils act as natural sinks for these elements (Shao et al., 2026), and when concentrations exceed threshold values, they may compromise ecosystem structure and function (Custodio et al., 2021; Hasi et al., 2025). Moreover, crops can absorb and translocate PTEs from the root zone to edible tissues, favoring their transfer along the soil-plant-food chain (Clemens and Ma, 2016; Paun et al., 2025). In addition, PTEs retained in soils may be re-entrained into the atmosphere or leached into aquatic systems, extending their environmental impact and increasing potential human exposure through inhalation, ingestion, and dermal contact (Yüksel et al., 2025). Recent studies indicate that these contaminants often originate from multiple interacting sources, including agricultural runoff, mining-related inputs, traffic emissions, industrial discharges, and other urban activities (Öncü et al., 2025; Tokatlı et al., 2026; Yüksel and Ustaoğlu, 2025).

Andean mountain systems constitute particularly relevant environments for studying these dynamics because of their marked altitudinal variability, geological diversity, and the coexistence of natural pedogenetic processes with strong anthropogenic pressures. Studies conducted along altitudinal gradients have shown that chemical properties, including metal and trace element contents, vary with elevation and with the associated climatic and pedogenetic conditions (Haque et al., 2023; Magnani et al., 2018), while land use and human activities further modify the concentration and spatial distribution of PTEs in agricultural landscapes (Anic et al., 2010). In Peru, these contrasts are framed by the division of the territory into three major natural regions, coast, highlands, and forest, where the coast concentrates much of the industrial, commercial, and agricultural activity, whereas the highlands are dominated by Andean systems in which small-scale farming is especially common (Velazco and Pinilla, 2018). In this context, the contrast is particularly evident between highland and coastal systems. In the Junín region, the Mantaro and Tarma valleys are characterized by mining activity (Villalobos Segura et al., 2023; Walter et al., 2021), which promotes the accumulation of PTEs in soils, while high vehicular traffic further contributes through atmospheric deposition of metallic particles. In contrast, coastal valleys such as Chancay and Pativilca are characterized by high agricultural productivity and continuous land use, where the sustained application of agricultural inputs, irrigation water quality, and the arid edaphoclimatic conditions of the coastal belt drive the accumulation and redistribution of elements in soils (Lopez and Camacho, 2022; Montagne et al., 2007; Rivera et al., 2011). These contrasting settings, mining-influenced highlands versus agriculturally intensive coastal lowlands provide a valuable natural framework for investigating how geochemical drivers, landscape structure, and human pressures interact to shape PTE distribution and associated ecological risk.

Despite growing interest in soil geochemistry across altitudinal gradients, comparative studies that simultaneously evaluate PTE spatial variability, multivariate geochemical structure, and ecological risk across contrasting agro-ecological systems within the same national context remain scarce. To address this gap, the present study analyzes the spatial variability of soil elemental composition in coastal and highland valleys of Peru, with particular emphasis on the distribution of PTEs including Cu, Cr, Fe, Mn, Mo, Ni, Pb, V, Zn, As, and Cd. Specifically, the objectives are: (i) to analyze the multivariate structure of PTEs across coastal and highland valleys; (ii) to compare spatial geochemical patterns between agricultural coastal and mining-influenced highland systems; and (iii) to quantify the relative contribution of edaphic, climatic, and topographic factors in structuring elemental composition and associated ecological risk. This study provides novel insights into the interplay between natural geochemical baselines and anthropogenic pressures in shaping PTE variability across contrasting Andean and coastal landscapes, with implications for soil quality assessment and environmental risk management.

2. Materials and methods

2.1. Study area

The study was conducted across four valleys in two contrasting agro-ecological regions of Peru: the central Pacific coast and the central Andes (Fig. 1). Coastal valleys (Pativilca and Chancay), located on the western Andean slope, are characterized by arid to semi-arid conditions, minimal annual precipitation (<50 mm yr^{-1}), and strong dependence on river-fed irrigation (Canaza et al., 2023; Rosas et al., 2023). Intensive irrigated agriculture is the predominant land use, and the sustained application of fertilizers, pesticides, and irrigation water of variable quality constitutes the primary driver of soil elemental dynamics in these systems (Lopez and Camacho, 2022; Montagne et al., 2007; Rivera et al., 2011). Highland valleys (Mantaro and Tarma), located in the Junín region at elevations ranging from 3,200 to over 4,000 m a.s.l., exhibit pronounced topographic variability, temperate to cold mountain climates, and greater seasonal precipitation (Carbajal et al., 2025; Rosas et al., 2023). Both valleys are strongly influenced by active and historical mining operations (Villalobos Segura et al., 2023; Walter et al., 2021), which may constitute major point sources of PTEs through tailings disposal, acid mine drainage, and the wind-driven dispersal of metal-bearing particle. In both regions, sampling sites were stratified into three altitudinal zones (high, middle, and low) to capture the full range of topographic and geochemical variability within each valley and to facilitate direct comparisons between the two contrasting systems (Fig. 1).

2.2. Soil sampling

Sampling areas within each basin were delineated using a 1,500 m buffer. Sampling locations were selected in QGIS 3.38 using the AcATaMa plugin (Llanos, 2024), applying a stratified random design based on agricultural and forest land-cover classes from the ESA WorldCover 2021 product (Zanaga et al., 2021). A total of 19, 22, 21, and 22 sampling points were established in Chancay, Pativilca, Mantaro, and Tarma, respectively, with a minimum inter-point distance of 200 m to ensure spatial independence. Within each valley, sites were stratified into high, middle, and lower altitudinal zones. Coastal sampling points are distributed along longitudinal river corridors in low-relief landscapes, whereas highland sites show greater spatial dispersion reflecting complex topography and environmental heterogeneity.

Samples were collected from homogeneous crop plots following an "X"-shaped design. A V-shaped excavation (20 cm depth) was made with a shovel, and a 2–3 cm thick slice was taken from one side, corresponding to the active root zone, following FAO and MINAM methodological guidelines (MINAM Guía Para Muestreo de Suelos, 2014; Mayor de San Simón, 2009).

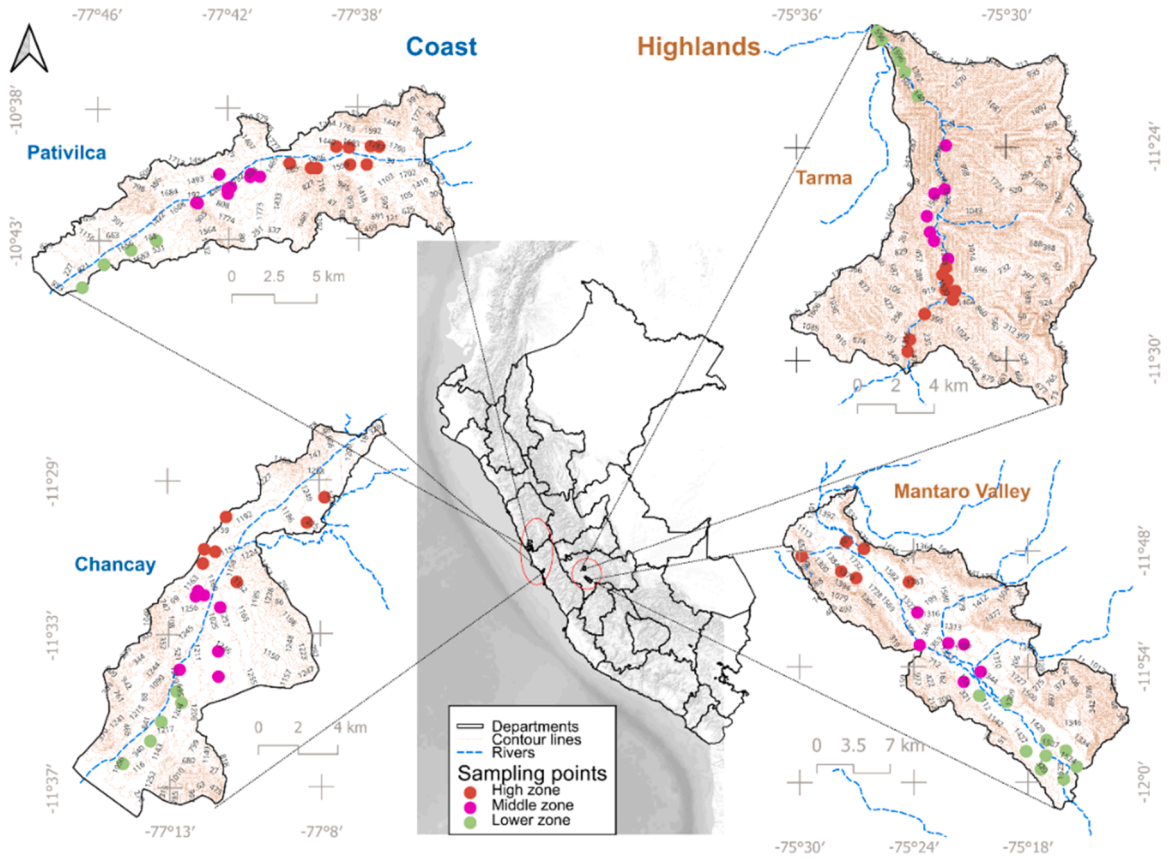

Fig. 1. Location of the coastal (Pativilca and Chancay) and highland (Mantaro and Tarma) study valleys in Peru, showing the stratification of sampling sites into high, middle, and lower altitudinal zones.

2.3. Soil physicochemical and elemental analysis

Samples were air-dried, disaggregated, homogenized, and sieved to 2 mm prior to analysis. Soil texture was determined by the Bouyoucos method (Beretta et al., 2014). Soil pH and electrical conductivity (EC) were measured in saturated paste extracts using an inoLab® pH 7310 and inoLab® Cond 7310, respectively. Total carbon (TC), total organic carbon (TOC), and total nitrogen (TN) were quantified by dry combustion with an elemental analyzer (LECO CN828, LECO Ltd., Germany). Extractable phosphorus (P_a) was determined using the Olsen method for neutral to alkaline soils and the Bray-1 method for acidic soils (Dari et al., 2019). Exchangeable cations (Ca^{2+}, Mg^{2+}, K^+, Na^+) and extractable potassium (K_a) were measured following ammonium saturation and analyzed by ICP-MS (Perkin Elmer NexION 2000, USA). Total elemental concentrations were determined following EPA Method 3051A (microwave-assisted acid digestion using an HNO_3–HCl, 9:3 acid mixture) (U.S. EPA, 2007) and EPA Method 6020B (ICP-MS) (U.S. EPA, 2014). All analyses were conducted at the Laboratorio de Suelos, Aguas y Foliares of the Instituto Nacional de Innovación Agraria (INIA), Lima, Peru.

2.4. Quality assurance and quality control (QA/QC)

QA/QC procedures were applied during sample preparation and instrumental analysis to ensure data reliability. Procedural blanks were included in each digestion batch and showed concentrations below the limit of detection (LOD) for all analytes, indicating negligible contamination. Instrument calibration was performed with multi-element standard solutions at four concentration levels, yielding correlation coefficients (R^2) above 0.999 for all analytes, and calibration verification using CCV standards showed recoveries ranging from 100.15 % to 106.00 % (Hernández-Mendoza et al., 2013). Analytical accuracy was assessed using the certified reference material ERA Metals in Soil PTCAT 620, with recoveries ranging from 99.70 % to 106.45 % for the reported elements. Internal standards (^{45}Sc, ^{74}Ge, ^{115}In, and ^{193}Ir) were used to correct for instrumental drift and matrix effects during ICP-MS analysis. Element-specific LOD, LOQ, CCV recovery, and reference material recovery values are provided in Supplementary Table AH. Overall, all QA/QC parameters were within acceptable limits for environmental trace element analysis.

2.5. Climatic variables

Key climatic variables were derived from satellite-based datasets. Mean annual temperature and precipitation were obtained from WorldClim 2.1 at 30 arc-second (~1 km) resolution, representing average conditions for 1970–2000 (Fick and Hijmans, 2017). Wind speed at 10 m height was retrieved from the Global Wind Atlas (GWA) 4.0 at 250 m spatial resolution (Davis et al., 2023).

2.6. Assessment of ecological risk indices

Ecological risk was assessed using six complementary indices: Contamination Factor (CF), Index of Geoaccumulation (Igeo), Pollution Load Index (PLI), Modified Contamination Degree (mCd), Potential Ecological Risk Index (RI), and Site Ranking Index (SRI). Geochemical background values were based on upper continental crust reference concentrations reported in previous studies, which were used here as a standardized comparative baseline because harmonized local background values are not currently available for all Peruvian agricultural valleys evaluated in this study (Taylor and Mclennan, 1995; Turekian et al., 1961). This approach has also been adopted in recent ecological risk studies conducted in Peru (Custodio et al., 2025; Custodio et al.,

2024). CF, Igeo, PLI, mCd, and SRI were calculated for Cu, Cr, Fe, Mn, Mo, Ni, Pb, V, Zn, As, and Cd. In contrast, the individual ecological risk factor (ERi) and RI were calculated only for elements with established toxic-response factors in the literature, following the Hakanson framework (Hakanson, 1980). Accordingly, toxicity-weighted risk calculations were applied to Cu, Cr, Ni, Pb, Zn, As, and Cd, whereas Fe, Mn, Mo, and V were retained only in the background-based contamination indices. The background values, toxic-response factors, and index-specific element selection used in this study are summarized in Supplementary Table AG. The individual ecological risk factor (E_r^i; Eq. (1)) and cumulative Potential Ecological Risk Index (RI; Eq. (2)) were calculated.

$$E_r^i = T_r^i \times CF_r^i \quad (1)$$

$$RI = \sum_{i=1}^{n} E_r^i \quad (2)$$

where $T_r^i$is the toxic response factor of each element. RI was classified as low (RI $\leq$ 95), moderate (95 $<$ RI $\leq$ 190), considerable (190 $<$ RI $\leq$ 380), or very high (RI $>$ 380). The PLI and mCd were derived from CF values as integrated indicators of overall site contamination. The Igeo was calculated following (Das et al., 2021; Muller, 1969) as a logarithmic function comparing the observed concentration with the background value adjusted by a correction factor of 1.5 to account for natural geochemical variability.

The SRI was computed from CF and Igeo values to enable cross-site contamination ranking (Omwene et al., 2018; Zhang et al., 2020). The weighted contamination index (W; Eq. (3)) and the SRI (Eq. (4)) were calculated as follows:

$$W = \frac{\sum n_i}{\sum i} \quad (3)$$

$$SRI = \frac{W}{S} \times 100 \quad (4)$$

SRI values were classified into four levels (Custodio et al., 2022): low (SRI $<$ median $-$ SD), moderate (median $-$ SD $\leq$ SRI $<$ median), high (median $\leq$ SRI $<$ median + SD), and severe (SRI $>$ median + SD).

2.7. Statistical and spatial structure analysis

All analyses were conducted in R (v4.0.5) (R Core Team, 2024). Data processing, cleaning, and organization were performed using the tidyverse, dplyr, and reshape2 packages (Wickham et al., 2019; Wickham et al., 2014), and graphical visualization was produced with ggplot2 (Wickham, 2016). Descriptive statistics (mean, median, standard deviation, and coefficient of variation) were calculated using the base stats package, and non-parametric comparisons among groups were conducted using the Kruskal–Wallis test.

Elemental concentrations were log-transformed where necessary to reduce skewness and stabilize variance. Pearson correlation analysis and clustered heatmaps were used to examine associations among soil physicochemical properties, climatic variables, and elemental concentrations (Benesty et al., 2009), generated using corrplot (Wei and Simko, 2010) and pheatmap (Kolde, 2010). PCA was applied to explore the multivariate structure of the dataset and identify dominant environmental gradients, using FactoMineR and factoextra (Lê et al., 2008). The multivariate analyses encompassed the eleven PTEs reported in Table 1, the additional trace elements summarized in Supplementary Table AE, and the climatic and soil physicochemical covariates reported in Supplementary Table AF. Differences in multivariate composition among valleys, zones, and crop types were assessed by PERMANOVA based on Bray–Curtis dissimilarities (999 permutations), complemented by PERMDISP to distinguish centroid shifts from differences in within-group variability (Anderson, 2001; Anderson, 2006; Jolliffe and Cadima, 2016). Variance partitioning via partial RDA was used to quantify the unique and shared contributions of soil physicochemical, climatic, and topographic/spatial predictor sets to elemental composition (Borcard et al., 1992), with adjusted R^2 values reported and significance assessed through permutation tests (999 permutations). Ecological risk indices were calculated through custom R scripts following their original mathematical formulations. Thematic cartography was developed in QGIS 3.36 (QGIS Development Team QGIS Development Team, 2024), where sampling points were georeferenced and maps were generated using graduated classification based on the defined index thresholds.

Table 1
Descriptive statistics (mean ± standard deviation) of soil physicochemical properties and potentially toxic element (PTE) concentrations across the four studied valleys.

Property / Element	Chancay	Pativilca	Mantaro	Tarma
Physicochemical Properties				
pH	7.66 ± 0.57	6.94 ± 0.32	7.21 ± 0.26	6.67 ± 0.47
EC (dS m^{-1})	2.10 ± 3.83	4.87 ± 4.32	1.76 ± 0.56	2.47 ± 1.50
Clay (%)	19.0 ± 3.12	32.6 ± 6.42	36.8 ± 10.4	28.8 ± 8.24
Silt (%)	18.1 ± 6.28	33.2 ± 9.86	30.0 ± 7.88	31.9 ± 7.63
Sand (%)	63.0 ± 5.46	34.2 ± 7.84	33.2 ± 12.9	39.3 ± 8.94
Potentially Toxic Elements (mg kg^{-1})				
Cu	44.6 ± 12.4	54.7 ± 12.6	96.3 ± 61.0	41.7 ± 11.9
Cr	33.6 ± 8.42	39.7 ± 10.5	49.2 ± 6.91	60.5 ± 46.0
Fe	3.21×10^4 ± 4.85×10^3	2.98×10^4 ± 5.44×10^3	4.87×10^4 ± 7.12×10^3	3.76×10^4 ± 6.21×10^3
Mn	496 ± 114	613 ± 102	822 ± 215	701 ± 187
Mo	1.12 ± 0.41	1.67 ± 0.52	2.34 ± 0.95	1.89 ± 0.74
Ni	10.1 ± 1.46	23.2 ± 4.56	33.9 ± 4.45	43.0 ± 25.7
Pb	30.9 ± 9.29	52.9 ± 15.2	169 ± 136	69.9 ± 90.3
V	60.8 ± 11.8	120 ± 12.5	101 ± 19.0	95.0 ± 33.0
Zn	122 ± 15.8	229 ± 46.8	842 ± 732	207 ± 98.6
As	25.6 ± 6.15	104 ± 14.0	162 ± 49.5	118 ± 42.2
Cd	0.694 ± 0.335	0.892 ± 0.318	0.041 ± 0.021	0.330 ± 0.254

EC: electrical conductivity; PTEs: potentially toxic elements. Values are expressed as mean ± standard deviation.

3. Results

3.1. Descriptive statistics

Table 1 presents the descriptive statistics (mean ± standard deviation) of the main soil physicochemical properties and elemental concentrations across the four studied valleys, revealing marked contrasts between coastal and highland systems.

Among coastal valleys, Chancay is characterized by predominantly sandy soils (63.0 ± 5.46 %), reflecting coarser parent materials and reduced capacity to retain trace elements. Pativilca shows higher silt and clay contents and the highest electrical conductivity (4.87 ± 4.32 dS m^{-1}), indicative of salt accumulation associated with arid conditions and intensive irrigation. Both coastal valleys exhibit comparatively lower elemental concentrations overall, with the exception of As, which reaches notable levels in Pativilca (104 ± 14.0 mg kg^{-1}).

Highland valleys show substantially higher concentrations of most PTEs and greater internal variability. The Mantaro Valley exhibits the highest clay content (36.8 ± 10.4 %) and the most elevated mean concentrations of Zn (842 ± 732 mg kg^{-1}), Pb (169 ± 136 mg kg^{-1}), Fe (4.87 × 10^4 ± 7.12 × 10^3 mg kg^{-1}), and Mn (822 ± 215 mg kg^{-1}). The large standard deviations associated with these elements suggest considerable spatial heterogeneity, likely reflecting lithological complexity and combined geogenic and anthropogenic inputs. Tarma presents elevated mean values of Cr (60.5 ± 46.0 mg kg^{-1}) and Ni (43.0 ± 25.7 mg kg^{-1}), with high dispersion in Pb (69.9 ± 90.3 mg kg^{-1}), pointing to spatial variability driven by local differences in parent material and

geomorphological dynamics. Cd concentrations contrast sharply between systems, being notably lower in Mantaro (0.041 ± 0.021 mg kg^{-1}) compared to coastal valleys, where values exceed 0.6 mg kg^{-1}. The descriptive statistics for the remaining trace elements, as well as for the climatic and soil physicochemical variables considered in the study, are presented in Supplementary Tables AE and AF, respectively.

3.2. Correlation analysis of edaphoclimatic properties and PTEs' concentrations

Pearson correlation analysis among soil physicochemical properties, climatic and spatial factors, and elemental concentrations is presented in Fig. 2. The clustered heatmap revealed three main groups of interrelated variables, reflecting distinct controlling processes within the agro-environmental system studied.

The first group comprised PTEs (Tl, Ba, Be, Mn, As, Zn, Pb, Sb, Cu, Ni, Cr, Co, and V), which exhibited strong positive intercorrelations ($r > 0.5$) and positive associations with clay and silt fractions, indicating a texture-mediated control linked to adsorption processes and mineral surface interactions. Moderate correlations with Fe and Mo further suggest the involvement of oxide and hydroxide phases in trace element retention, consistent with well-documented geochemical partitioning mechanisms in metal-enriched soils.

The second group included soil properties associated with fertility and buffering capacity, namely CEC, exchangeable bases (Ca, Mg, K), total and organic carbon, $CaCO_3$, and major cations, which showed strong internal correlations ($r > 0.6$) and positive associations with precipitation and elevation. This pattern highlights the influence of climatic and topographic gradients on soil development and nutrient accumulation, particularly along the altitudinal gradient that characterizes the highland valleys.

The third group integrated slope, pH, Mg, Ag, and Cd, variables that generally showed weak correlations with the remaining properties. The co-occurrence of Cd and Ag within this cluster suggests a distinct geochemical behavior, potentially reflecting greater mobility under specific pH and drainage conditions of the sampled sites, and warrants further investigation into their source and fate across the studied systems.

3.3. Zonal variability in elemental concentrations within valleys

To complement the correlation structure, elemental concentration distributions were examined by valley and altitudinal zone (Fig. 3). Overall, zonal contrasts within valleys were modest, though the elements used for ecological risk assessment (Cu, Cr, Fe, Mn, Mo, Ni, Pb, V, Zn, As, and Cd) showed the most ecologically relevant differences across

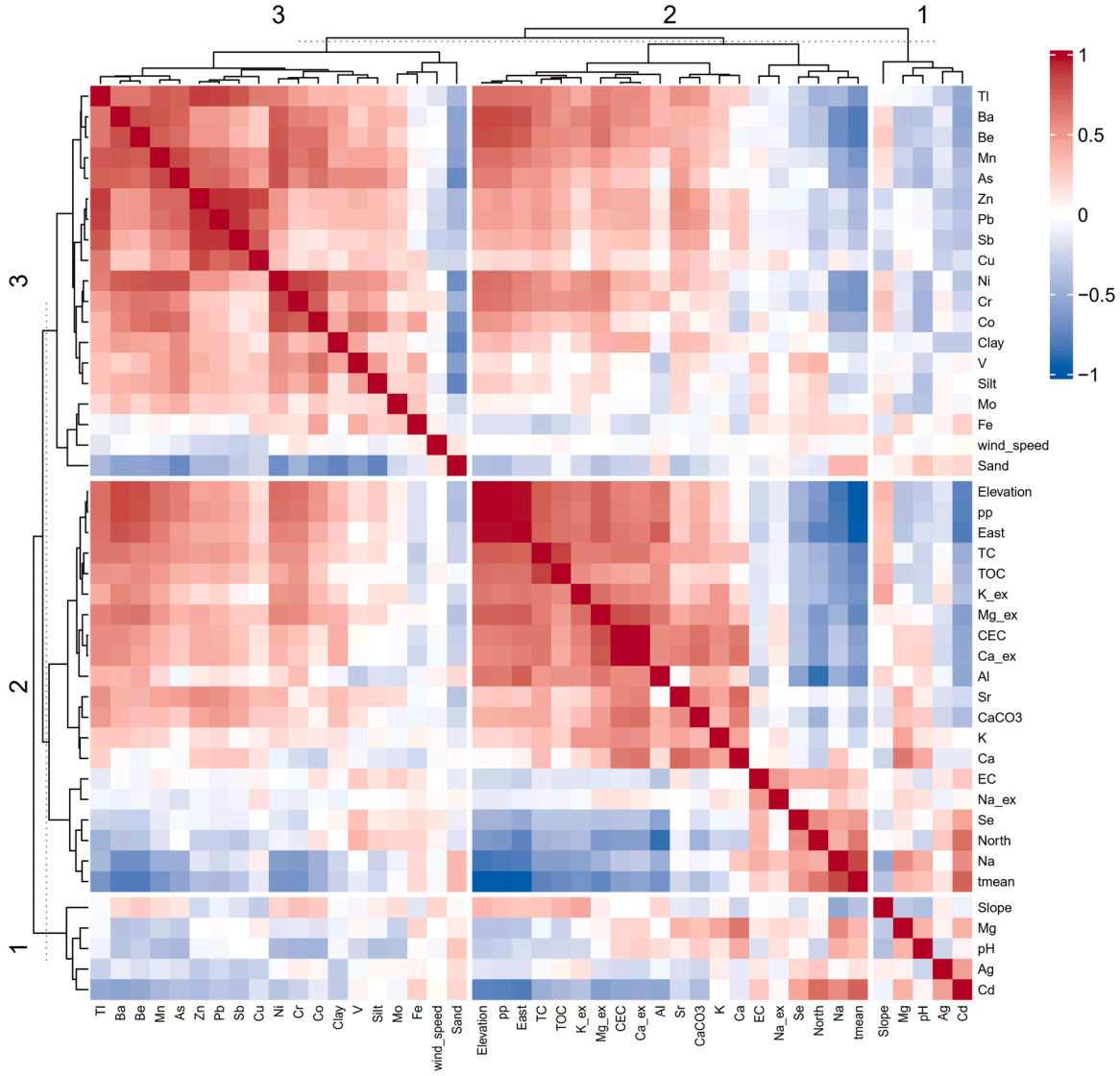

Fig. 2. Clustered correlation heatmap of soil physicochemical properties, climatic and spatial factors, and elemental concentrations across the studied valleys.

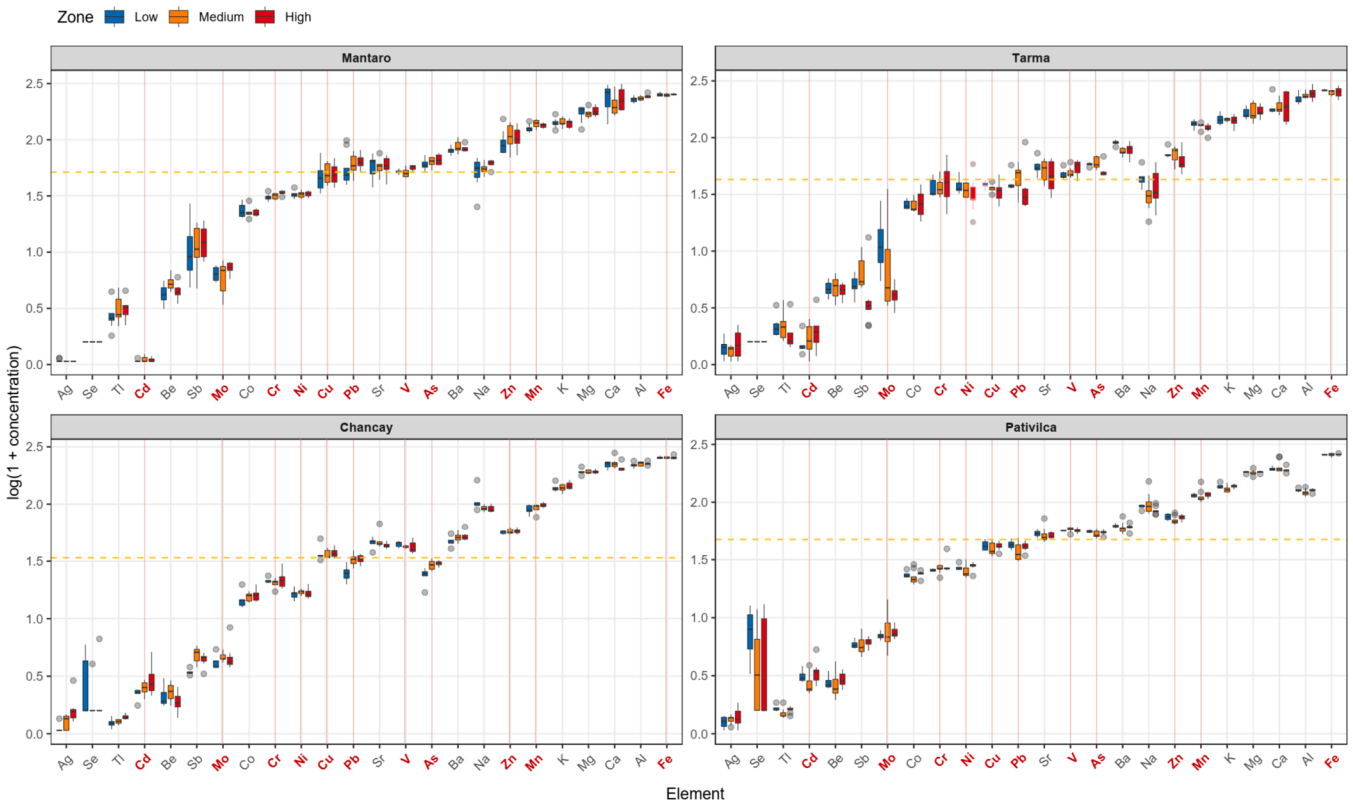

Fig. 3. Elemental concentrations by valley and altitudinal zone. Boxplots show log-transformed concentrations [log(1 + concentration)] for low, medium, and high zones. The dashed line indicates the mean concentration across all elements. Elements used in the ecological risk assessment (Cu, Cr, Fe, Mn, Mo, Ni, Pb, V, Zn, As, and Cd) are highlighted in red on the x-axis. Boxes represent interquartile ranges, central lines denote medians, and points indicate individual observations.

the low, medium, and high zones.

Among these elements, the most pronounced zonal variation was observed for As, Pb, Cu, and Zn, where differences between low and high zones in log-transformed scale (approximately 0.1 to 0.2 log units) correspond to meaningful proportional increases in original concentrations. Highland valleys, particularly Mantaro and, to a lesser extent, Tarma, consistently exhibited higher median concentrations and greater dispersion than their coastal counterparts.

Among non-risk elements, zonal contrasts were generally limited. Fe, Al, and Ca displayed minimal zonal variation (<0.1 log units), while Mn, V, and Ni showed consistent but small shifts across zones. These patterns suggest that major pedogenic elements are more homogeneously distributed within valleys, whereas the ecological risk elements are more sensitive to local altitudinal and anthropogenic gradients, reinforcing the role of elevation and land-use history as key drivers of spatial elemental variability.

3.4. Multivariate ordination of soil, climatic, spatial, and elemental variables

The PCA biplot (Fig. 4) integrates soil physicochemical properties, climatic and spatial variables, and elemental concentrations. The first two components explained 50.2 % of total variance (PC1: 36.8 %; PC2: 13.4 %), adequately representing the main gradients of variability in the ordination space.

PC1 defined a soil-geochemical gradient, with strong positive loadings for clay, silt, CEC, exchangeable cations (Ca, Mg, K), total and organic carbon, and the ecological risk elements As, Pb, Zn, Ni, Cr, Mn, Co, and V. Negative PC1 scores were associated with sand content, pH, and $CaCO_3$, reflecting the contrasting behavior of coarser-textured, lower-adsorption-capacity soils. PC2 represented a climatic-spatial gradient driven by geographical coordinates (North, East), mean temperature, wind speed, and elevation, capturing the influence of spatial position and local climatic conditions on elemental variability.

In the ordination space, samples grouped consistently by valley, with coastal valleys (Chancay and Pativilca) occupying negative PC1 scores and highland valleys (Mantaro and Tarma) projecting toward positive PC1, reflecting higher PTE concentrations and finer textures. Zonal differentiation introduced secondary within-valley variability, particularly evident in Mantaro, where the high zone extended furthest along the positive PC1 axis.

3.5. Multivariate group structure: PERMANOVA and PERMDISP

To assess whether valley and zone significantly structured elemental composition, PERMANOVA and PERMDISP tests were applied to the Bray–Curtis dissimilarity matrix. The Valley × Zone interaction explained a small but statistically significant proportion of the compositional variation ($R^2 = 0.049$, $F = 2.09$, $p = 0.011$) (Table 2). When crop type was incorporated into the model, its effect was not significant ($R^2 = 0.068$, $p = 0.838$), while the Valley × Zone interaction became marginal ($R^2 = 0.037$, $p = 0.086$) and residual variation increased, indicating that crop type does not constitute a dominant structuring factor at the scale evaluated.

To evaluate whether land-use category exerted an independent influence beyond spatial controls, a complementary PERMANOVA including land-use group, Valley, and Zone was fitted (Table 3). After accounting for spatial structure, land-use group was not significant ($R^2 = 0.013$, $p = 0.414$), whereas Valley remained the dominant factor ($R^2 = 0.488$, $F = 38.36$, $p = 0.001$). Zone was also non-significant ($R^2 = 0.010$, $p = 0.256$), confirming that elemental composition is primarily structured by geographic context rather than by current agricultural management practices. Across both models, Valley consistently emerged as the principal structuring factor, with land use and intra-valley zonation

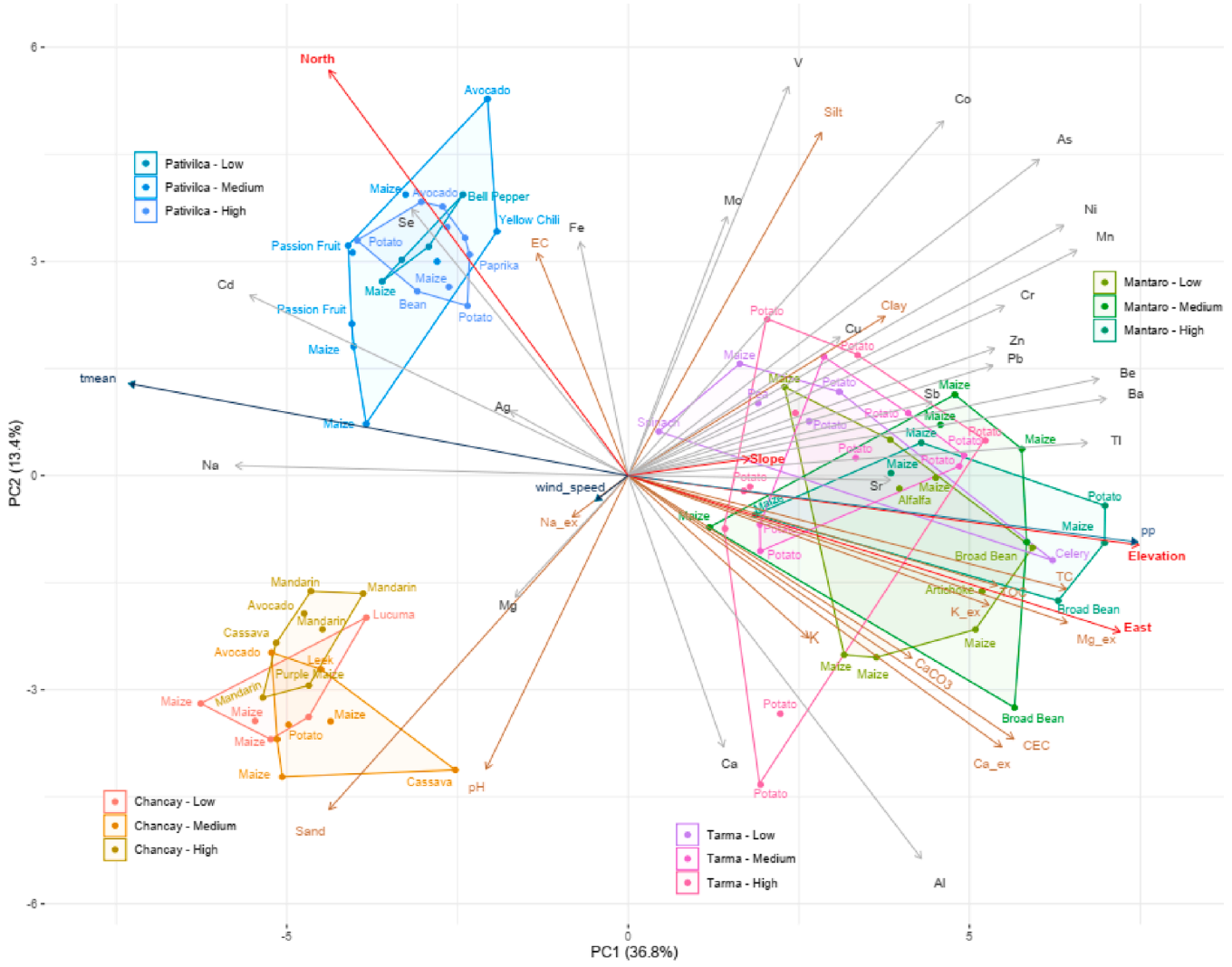

Fig. 4. PCA biplot integrating soil physicochemical properties, climatic and spatial variables, and elemental concentrations, with convex hulls delineating valley-zone groups and crop-level distributions.

Table 2
PERMANOVA results based on Bray–Curtis dissimilarity.

Model	Factor	df	Sum of squares	R^2	F	*p*-value
Valley × Zone	Valley × Zone	6	0.00485	0.049	2.09	**0.011**
	Residual	72	0.02779	0.282		
	Total	83	0.09851	1.000		
Valley × Zone + Crop	Crop	20	0.00673	0.068	0.83	0.838
	Valley × Zone	6	0.00365	0.037	1.50	0.086
	Residual	52	0.02105	0.214		
	Total	83	0.09851	1.000		

Table 3
PERMANOVA testing the effects of land-use group and spatial factors on elemental composition.

Factor	df	Sum of squares	R^2	F	p-value
Land-use group	3	0.00129	0.013	1.03	0.414
Valley	3	0.04810	0.488	38.36	0.001
Zone	2	0.00103	0.010	1.23	0.256
Residual	75	0.03134	0.318		
Total	83	0.09851	1.000		

Table 4
Homogeneity of multivariate dispersion (PERMDISP) results for elemental composition.

Grouping factor	df	F	*p*-value
Valley	3	11.40	**0.001**
Valley–Zone	11	2.53	**0.012**

PERMDISP results (tests of homogeneity of multivariate dispersions).

contributing negligible independent explanatory power.

Homogeneity of multivariate dispersion tests (PERMDISP) revealed significant differences in within-group variability among valleys ($F = 11.40$, $p = 0.001$). When Valley–Zone combinations were considered, dispersion differences remained significant but with a markedly lower F-value ($F = 2.53$, $p = 0.012$) (Table 4). These results indicate that valleys differ not only in their compositional centroids but also in their degree of internal elemental heterogeneity. Because significant PERMDISP can contribute to a significant PERMANOVA F-statistic independently of true centroid displacement, group differences should be interpreted with caution. However, the high explanatory power of Valley ($R^2 = 0.488$, $F = 38.36$) suggests that the observed compositional separation reflects genuine differences among valleys rather than dispersion artefacts

alone. The reduction in the PERMDISP F-value under finer spatial subdivision (F = 2.53 vs. F = 11.40) is consistent with the presence of localized geochemical gradients within valleys.

3.6. Variance partitioning of elemental composition

Variance partitioning via partial RDA quantified the individual and shared contributions of soil physicochemical properties, climatic variables, and spatial/topographic factors to multivariate elemental composition (Fig. 5). Together, the three predictor sets explained approximately 60 % of total variation (adjusted $R^2 = 0.597$), with 40.3 % remaining unexplained, reflecting the inherent complexity of soil geochemical systems and the potential influence of unmeasured local factors.

The unique effects of individual predictor sets were comparatively small. Soil physicochemical properties explained 1.0 % of variance independently, and its pure effect was not statistically significant once climate and spatial structure were controlled for (F = 1.16, p = 0.205). The pure climatic effect accounted for 5.4 % of variance and was highly significant (F = 4.01, p = 0.001), while the pure spatial/topographic effect explained 3.6 % and was also significant (F = 2.53, p = 0.003) (Table 5).

In contrast, shared fractions dominated the explained variance, highlighting the strong coupling among predictor sets. The shared effect between climate and spatial/topographic variables accounted for 10.7 % of variance, the soil and spatial/topographic shared fraction explained 7.3 %, and the soil and climate shared fraction contributed 3.5 %. Notably, the three-way shared fraction among all predictor sets was the largest single component, explaining 28.1 % of variance, indicating that soil properties, climatic gradients, and spatial/topographic context operate in a tightly integrated manner rather than as independent drivers.

Overall, these results indicate that climate and spatial/topographic factors exert statistically significant independent influences on elemental composition, whereas soil physicochemical properties contribute primarily through their shared variation with the other predictors. This pattern is consistent with the correlation structure, zonal distributions, and ordination results presented in the preceding sections, and reinforces the interpretation that elemental distributions across these valleys are governed by interacting environmental controls operating at multiple spatial scales.

3.7. Integrated ecological risk across coastal and highland valleys

The spatial distribution of the Pollution Load Index (PLI), which reflects the overall pollution condition of a site, and the Modified Contamination Degree (mCd), which represents an overall indicator of contamination, across the four studied valleys is shown in Fig. 6. In the highland valleys of Mantaro and Tarma, a substantial proportion of sites fell within the environmental deterioration category according to PLI, and mCd values reached very high and extremely high contamination levels. These elevated values showed a spatial pattern aligned with the geomorphological configuration of the valleys, suggesting spatial heterogeneity consistent with the spatial and climatic controls identified in the multivariate and variance partitioning analyses. In contrast, the coastal valleys of Pativilca and Chancay were predominantly characterized by slight contamination according to PLI, while mCd indicated moderate to high contamination levels with a relatively uniform spatial distribution. This pattern suggests a more diffuse accumulation process associated with sustained agricultural intensification and permanent irrigation systems, rather than localized geochemical inputs.

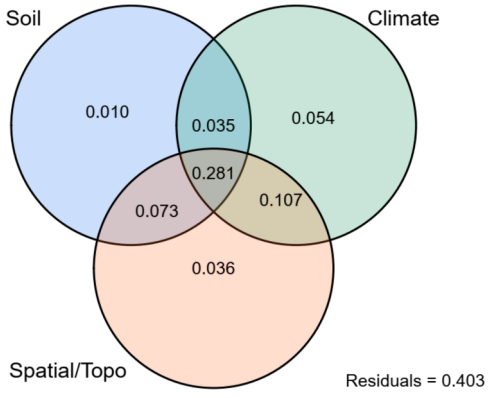

Fig. 5. Variance partitioning of elemental composition explained by soil, climatic, and spatial/topographic factors.

Table 5
Partial redundancy analysis (RDA): permutation tests for unique predictor effects.

Predictor set (pure effect)	df	Variance	F	p-value
Soil physicochemical	12	0.000347	1.16	0.205
Climate	3	0.000299	4.01	0.001
Spatial / topographic	4	0.000251	2.53	0.003

Note: Each predictor set was tested while controlling for the remaining two sets.

The ecological risk classification based on the Site Ranking Index (SRI), disaggregated by crop, valley, and altitudinal zone, further shows this spatial differentiation (Fig. 7). In the coastal valleys, most sampled crops fell within low to moderate risk categories across the three zones, with limited dispersion toward high or severe levels, suggesting a relatively more homogeneous spatial distribution of PET accumulation under intensive agricultural management. In contrast, the highland valleys showed higher SRI values and greater variability among sites and crops. In Mantaro, several crops in the lower and middle zones reached high and severe risk categories, while Tarma showed a similar pattern, particularly in the middle and high zones. Within the highland systems, risk values tended to concentrate toward the upper end of the scale across different crops and topographic zones, suggesting that broader spatial and environmental controls may exert a stronger influence on PET concentrations than crop-specific effects, consistent with the non-significant land-use effects identified in the PERMANOVA analysis.

Element-wise analyses revealed limited and element-specific responses to management practices. As and Pb did not differ significantly among land-use groups (p = 0.102 and p = 0.108, respectively), whereas Cd exhibited a highly significant effect ($p < 0.001$) and Zn showed a weaker but significant difference (p = 0.041). Complementarily, the Nemerow pollution index by Valley–Zone combination showed median values ranging from 0.94 to 1.37, corresponding to low to moderate contamination levels, with significant differences confirmed by Kruskal–Wallis test ($\chi^2 = 45.81$, df = 11, $p < 0.001$), indicating that ecological risk follows the same spatial organization identified throughout the multivariate analyses.

4. Discussions

4.1. Spatial structuring of elemental composition across valleys

The predominance of the Valley factor over Zone or crop type is consistent with studies showing that multielement patterns in agricultural soils are controlled by broad-scale geographic and environmental gradients rather than by current land-use categories (Rate, 2021; Sun et al., 2013), where geology, topography, and climate generate coherent regional elemental associations (Han et al., 2019; Yavitt et al., 2009). Accordingly, elemental composition in the studied valleys was mainly structured by valley-scale differences, whereas the effects of land-use group and Zone were not significant. In agricultural and peri-agricultural systems, internal heterogeneity is closely linked to geomorphological configuration and parent material distribution, where regional

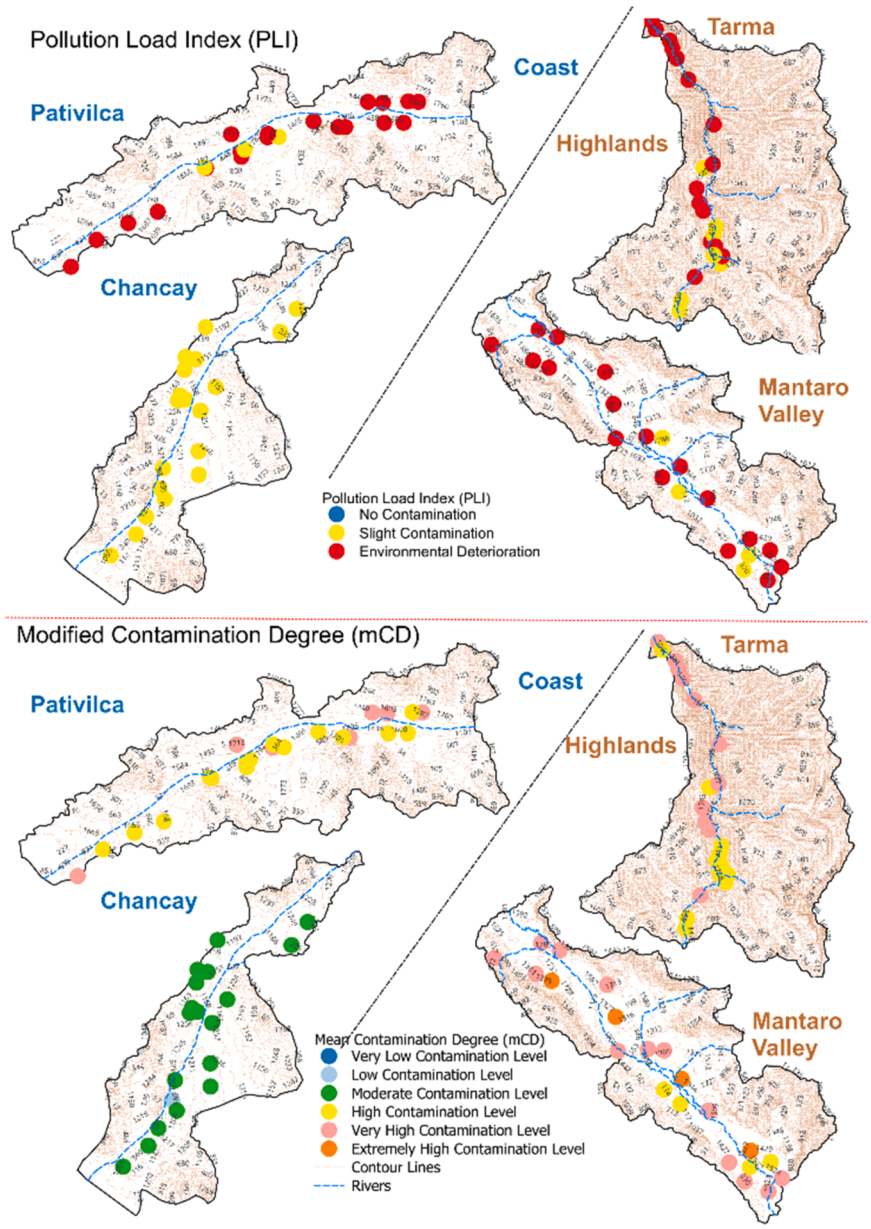

Fig. 6. Spatial distribution of the Pollution Load Index (PLI) and Modified Contamination Degree (mCD) in agricultural soils across coastal and highland valleys.

spatial organization explains a substantial proportion of edaphic and geochemical variability (Cui et al., 2025; Nyengere et al., 2023). The absence of a significant land-use effect does not imply the absence of anthropogenic influence, but rather that such effects operate at a subordinate scale relative to the dominant spatial framework (Alharbi et al., 2025). In heterogeneous landscapes, anthropogenic signals are typically superimposed upon a prevailing geogenic background without reorganizing the overall multielement assemblage (Jia et al., 2024; Rate, 2021; Sun et al., 2013). This spatial differentiation is further supported by evidence that topographic and environmental gradients modulate not only elemental concentrations but also the magnitude and variability of associated ecological risk (Cui et al., 2025; Li et al., 2022; Ritz et al., 2004; Yavitt et al., 2009).

4.2. Environmental drivers and shared controls: insights from variance partitioning

The three predictor sets jointly explained approximately 60 % of total elemental variation, consistent with studies showing that macro-environmental, spatial, and edaphic drivers together account for substantial proportions of ecological variability in complex environmental systems (Anderson and Cribble, 1998; Paranavithana et al., 2023; Qi et al., 2025). Pure effects were relatively small, particularly for soil physicochemical properties (1 %), whereas climate (5 %) and spatial/topographic factors (4 %) showed statistically significant independent effects. Topography has been widely identified as a key determinant of metal variability, with elevation and slope influencing the redistribution of fine particles and associated metals (Nyengere et al., 2023; Wu et al., 2021), and heavy metal concentrations in soils from mining-influenced regions peaking at higher altitudes possibly due to topographic barriers (Ding et al., 2017).

The most relevant outcome, however, was the dominance of shared fractions, particularly the three-way fraction among soil, climate, and topography (28 %), indicating strong structural coupling among predictor sets (Paranavithana et al., 2023; Wu et al., 2023). This pattern suggests that elemental composition emerges from the interaction among climatic gradients, topographic configuration, and pedogenic processes rather than from any single controlling factor (Jia et al.,

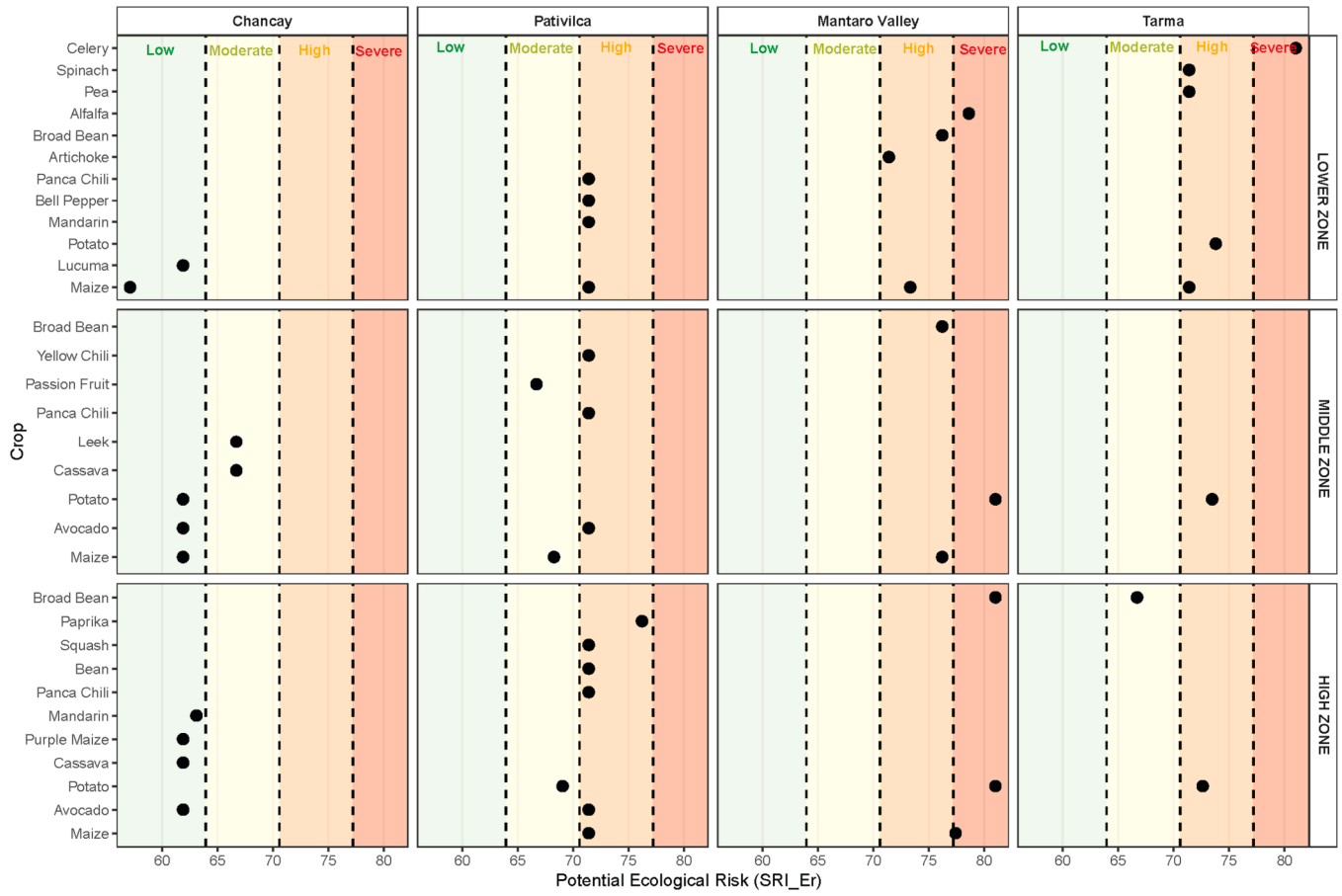

Fig. 7. Ecological risk classification (SRI) in agricultural soils across coastal and highland valleys.

2024). The unexplained fraction (40 %) likely reflects local processes and site-specific inputs not captured by the selected predictors (Sun et al., 2013; Wu et al., 2021), reinforcing the idea that soil properties contribute primarily through their covariation with broader environmental gradients. Likewise, previous studies in this highland region have reported elevated heavy metal concentrations in soils that have been associated with both natural geologic sources and historical mining activities, although direct source attribution was not performed in the present study (Vargas et al., 2022).

4.3. Limited role of crop type and land-use categories

The absence of a significant multivariate effect of crop type and land-use categories indicates that agricultural management does not constitute the primary structuring factor of elemental composition at the scale considered here. This finding is consistent with evidence showing that topographic and terrain-related variables outweigh surface management practices in explaining spatial patterns of heavy metals, particularly in landscapes with pronounced geomorphological gradients (Qi et al., 2025; Wu et al., 2021) . Crop type alone does not generate sufficient geochemical differentiation to override broader environmental controls, and land-use effects, where present, tend to produce localized accumulations or element-specific responses rather than reorganizing the overall multielement assemblage (Jia et al., 2024; Sun et al., 2013).

Scale represents a critical factor in interpreting these results. At broader regional extents, environmental gradients tend to overshadow local management effects (Anderson and Cribble, 1998), and strong spatial autocorrelation in soil chemical properties further constrains the expression of management effects at finer scales (Nyengere et al., 2023). From a management perspective, agricultural interventions may influence specific elements under certain conditions, but typically interact with pre-existing environmental controls rather than replacing them (Tang et al., 2024; Zhang et al., 2025). Consequently, strategies aimed at mitigating elemental accumulation should account for the dominant role of climate and topography in structuring soil geochemistry rather than assuming uniform responses across land-use categories.

4.4. Integrated ecological risk patterns across coastal and highland systems

Composite indices (PLI, mCd, SRI, and Nemerow) revealed greater risk intensity and spatial heterogeneity in highland valleys than in coastal systems, consistent with studies showing that integrated indices effectively capture the magnitude and complexity of ecological risk (Alharbi et al., 2025; Ritz et al., 2004). The elevated risk levels observed in highland systems are consistent with the combined influence of geomorphological gradients, altitudinal and erosional processes, and regional geochemical conditions described in previous studies (Han et al., 2019; Li et al., 2026); however, as no formal source apportionment was conducted, these factors should be regarded as plausible contextual explanations rather than demonstrated sources. The Nemerow index proved particularly sensitive to dominant elements that elevate overall integrated risk even when other metals remain at moderate levels (Ritz et al., 2004; Song et al., 2018), while the greater severity observed in Mantaro and Tarma was also consistent with evidence highlighting the role of topographic complexity in shaping ecological risk patterns (Sun et al., 2013; Tang et al., 2024).

Coastal systems exhibited more homogeneous patterns characterized by slight to moderate contamination according to PLI and mCd, which may reflect diffuse accumulation processes consistent with long-term

agricultural management and spatially distributed inputs, though the specific sources responsible for these patterns cannot be directly attributed without source apportionment analysis. Similar patterns have been reported in agricultural regions under long-term management and spatially distributed atmospheric deposition, where gradual but relatively uniform increases in metal concentrations may occur (Wu et al., 2023; Zhang et al., 2025). In such contexts, risk variability tends to be lower than in systems affected by more localized high-intensity pressures (Qi et al., 2025; Zhang et al., 2019), and the combined use of multiple indices has been recommended to prevent underestimation of ecological risk in scenarios of moderate but persistent contamination (Ritz et al., 2004; Santos-Francés et al., 2017). In addition, background metal values may vary across locations due to site-specific processes such as weathering and erosion (Yüksel and Ustaoğlu, 2025).

The health risk implications of the PTE concentrations detected in this study merit consideration alongside the ecological risk indices. Elements such as As, Cr, Ni, and Pb, which showed elevated concentrations particularly in highland valleys, are recognized as priority contaminants due to their carcinogenicity and capacity to reach human populations through multiple exposure pathways, including ingestion of contaminated soil particles, consumption of crops grown on affected soils, and inhalation of resuspended dust (Hou et al., 2025). Recent assessments in comparable urban and peri-urban settings have demonstrated that these pathways can generate non-carcinogenic and carcinogenic risks exceeding acceptable thresholds, particularly for children, with Cr, Ni, and As identified as the main contributors (Yüksel et al., 2025).

4.5. Implications for environmental monitoring and soil management

The results indicate that environmental monitoring frameworks should explicitly incorporate climatic and topographic variables alongside soil physicochemical properties, as variation partitioning and multivariate analyses consistently demonstrate that macro-environmental and spatial components explain a greater proportion of elemental variability than local management factors (Anderson and Cribble, 1998; Paranavithana et al., 2023). Monitoring schemes based solely on land-use classifications risk underestimating the hierarchical influence of broader environmental controls (Nyengere et al., 2023; Qi et al., 2025; Wu et al., 2021). In this regard, atmospheric deposition has been shown to facilitate metal dispersion far beyond mining sites, impacting populated areas and vulnerable ecosystems at regional scales (Muñoz et al., 2013).

In highland systems, where ecological risk indices reveal greater intensity and spatial heterogeneity, monitoring efforts should prioritize sectors associated with pronounced topographic gradients and geochemical conditions potentially linked to geogenic or mining-related inputs, recognizing that the relative contribution of these sources requires dedicated source apportionment studies for formal confirmation (Han et al., 2019; Li et al., 2026; Sun et al., 2013), incorporating geomorphological variables to account for slope-driven erosion and metal redistribution processes (Qi et al., 2025; Wu et al., 2021). In coastal systems, characterized by diffuse accumulation patterns, long-term surveillance approaches focused on detecting gradual enrichment trends are more appropriate than hotspot-based strategies (Wu et al., 2023; Zhang et al., 2025). In both contexts, the combined use of multiple contamination indices is recommended to prevent underestimation of ecological risk under conditions of moderate but persistent contamination (Ritz et al., 2004; Santos-Francés et al., 2017).

In agricultural contexts, the soil-plant transfer pathway constitutes an additional critical dimension of environmental risk, as crops can absorb and translocate PTEs from the root zone to edible tissues, extending the potential for human exposure along the food chain. Studies conducted specifically in the highland areas of the Peruvian Andes have demonstrated that soils near metallurgical complexes show Pb concentrations exceeding maximum limits for agricultural soil by more than threefold, with measurable transfer through the soil-root-shoot system documented in grassland species (Castro-Bedriñana et al., 2021). In the Mantaro Valley specifically, foliar concentrations of Cd, Pb, and As in crops such as potato, broad bean, and quinoa have been reported to exceed Codex Alimentarius limits, with bioaccumulation factors greater than one recorded for several species, and irrigation further increasing metal bioavailability and foliar accumulation (Ccopi et al., 2026). These findings reinforce the importance of integrating food safety considerations into environmental monitoring frameworks for the agricultural valleys evaluated here, particularly in highland systems where ecological risk indices indicate greater contamination intensity.

5. Conclusions

The spatial variability of soil elemental composition across coastal and highland valleys of Peru is predominantly governed by interacting environmental gradients, particularly climatic and topographic factors, rather than by crop type or current land-use categories. Variance partitioning confirmed that shared environmental effects dominate over pure predictor contributions, reflecting the strong coupling among pedogenic, climatic, and spatial processes that structure elemental distributions at the regional scale.

Ecological risk assessment revealed a clear contrast between systems. Highland valleys presented greater contamination intensity, spatial heterogeneity, and more frequent high-risk categories, which may reflect the combined influence of geogenic sources, mining-related inputs, and topographic complexity. Coastal valleys showed more homogeneous and diffuse accumulation patterns, which may be related to long-term agricultural intensification under arid conditions. In both systems, the soil-plant transfer pathway represents an additional dimension of concern, as evidenced by reported exceedances of Codex Alimentarius limits for Cd, Pb, and As in crops cultivated in the Mantaro Valley, underscoring the food safety implications of the contamination levels documented here.

These results emphasize that environmental monitoring and soil management strategies should incorporate regional climatic and topographic structure alongside soil physicochemical properties, and that food safety surveillance should be integrated into monitoring frameworks for highland agricultural systems. The combined use of multiple contamination indices is recommended to ensure adequate characterization of ecological risk across contrasting agro-ecological systems.

Ethics statement

Not applicable: This manuscript does not include human or animal research.

Funding

This research was funded by the INIA project “Mejoramiento de los servicios de investigación y transferencia tecnológica en el manejo y recuperación de suelos agrícolas degradados y aguas para riego en la pequeña y mediana agricultura en los departamentos de Lima, Áncash, San Martín, Cajamarca, Lambayeque, Junín, Ayacucho, Arequipa, Puno y Ucayali” CUI 2487112, of the Ministry of Agrarian Development and Irrigation (MIDAGRI) of the Peruvian Government.

CRediT authorship contribution statement

Wendy E. Pérez: Writing – review & editing, Visualization, Methodology, Investigation, Data curation, Conceptualization. **Dennis Ccopi:** Writing – original draft, Validation, Software, Methodology, Formal analysis. **Ricardo Flores-Marquez:** Writing – review & editing, Writing – original draft, Validation, Investigation, Conceptualization. **Carlos Carbajal:** Writing – original draft, Visualization, Validation,

Investigation, Conceptualization. **Samuel Pizarro:** Software, Methodology, Formal analysis, Data curation, Conceptualization.

Declaration of competing interest

The authors declare that they have no known competing financial interests or personal relationships that could have appeared to influence the work reported in this paper.

Supplementary materials

Supplementary material associated with this article can be found, in the online version, at doi:10.1016/j.envadv.2026.100714.

Data availability

Data will be made available on request.

References

Alharbi, T., El-Sorogy, A.S., Rikan, N., 2025. A GIS and multivariate analysis approach for mapping heavy metals and metalloids contamination in landfills: a case study from Al-Kharj, Saudi Arabia. Land (Basel) 14, 1697. https://doi.org/10.3390/land14081697.

Anderson, M.J., Cribble, N.A., 1998. Partitioning the variation among spatial, temporal and environmental components in a multivariate data set. Aust. J. Ecol. 23, 158–167. https://doi.org/10.1111/j.1442-9993.1998.tb00713.x.

Anderson, M.J., 2001. A new method for non-parametric multivariate analysis of variance. Austral. Ecol. 26, 32–46. https://doi.org/10.1111/j.1442-9993.2001.01070.pp.x.

Anderson, M.J., 2006. Distance-based tests for homogeneity of multivariate dispersions. Biometrics 62, 245–253. https://doi.org/10.1111/j.1541-0420.2005.00440.x.

Anic, V., Hinojosa, L.F., Díaz-Forester, J., Bustamante, E., de la Fuente, L.M., Casale, J.F., de la Harpe, J.P., Montenegro, G., Ginocchio, R., 2010. Influence of soil chemical variables and altitude on the distribution of high-alpine plants: the case of the andes of Central Chile. Arct. Antarct. Alp. Res. 42, 152–163. https://doi.org/10.1657/1938-4246-42.2.152.

Bauer, T., Kirichkov, M., Polyakov, V., Kravchenko, E., Butova, V., Chernikova, N., Jabborova, D., Minkina, T., 2026. Metal–organic framework modified biochar nanocomposite for sustainable stabilization of heavy metals in contaminated soils. Environ. Nanotechnol. Monit. Manag. 25, 101132. https://doi.org/10.1016/j.enmm.2026.101132.

Bautista-Cruz, A.; Arnaud-Viñas, M. del R.; Carrillo-González, R. Trace elements concentration in two agricultural areas. 2011.

Benesty, J.; Chen, J.; Huang, Y.; Cohen, I. Pearson correlation coefficient. In; 2009; pp. 1–4.

Beretta, A.N., Silbermann, A.V., Paladino, L., Torres, D., Bassahun, D., Musselli, R., García-Lamohte, A., 2014. Soil texture analyses using a hydrometer: modification of the Bouyoucos method. Cienc. Investig. Agrar. 41, 25–26. https://doi.org/10.4067/S0718-16202014000200013.

Binde, D.R., de Moraes, M.F., Haefele, S.M., Pierangeli, M.A.P., 2025. Impact of agricultural activities on trace element levels in soils of Mato Grosso, Brazil. Chemosphere 384, 144497. https://doi.org/10.1016/j.chemosphere.2025.144497.

Borcard, D., Legendre, P., Drapeau, P., 1992. Partialling out the spatial component of ecological variation. Ecology 73, 1045–1055. https://doi.org/10.2307/1940179.

Canaza, D., Calizaya, E., Chambi, W., Calizaya, F., Mindani, C., Cuentas, O., Caira, C., Huacani, W., 2023. Spatial distribution of soil organic carbon in relation to land use, based on the weighted overlay technique in the high andean ecosystem of Puno—Peru. Sustainability 15, 10316. https://doi.org/10.3390/su151310316.

Carbajal, C., Tumbalobos-Dextre, M., Condori-Ataupillco, T., Cuellar-Condori, N., Gavilan, C., 2025. Spatial prediction of soil organic carbon stocks across contrasting Andean Basins, Peru. Geoderma Reg. 43, e01026. https://doi.org/10.1016/j.geodrs.2025.e01026.

Castro-Bedriñana, J., Chirinos-Peinado, D., Garcia-Olarte, E., Quispe-Ramos, R., 2021. Lead transfer in the soil-root-plant system in a highly contaminated andean area. PeerJ 9, e10624. https://doi.org/10.7717/peerj.10624.

Ccopi, D., Requena-Rojas, E., Ortega, K., Solórzano-Acosta, R., Révolo-Acevedo, R., Pizarro, S., 2026. Bioaccumulation of heavy metals in high andean crops of the Peruvian andes: comparative evaluation between irrigated and dry systems. J. Agric. Food Res. 25, 102575. https://doi.org/10.1016/j.jafr.2025.102575.

Chand, V., Islam, A.R.M.T., Mia, M.Y., Islam, M.S., Al Masud, M.A., Khan, R., Pal, S.C., Singh, S.K., Deo, R.R, 2024. Investigating soil physicochemical factors influencing trace element contamination at the semi-urban-rural home gardening interfaces on the Fiji Islands. Geoderma Reg. 39, e00884. https://doi.org/10.1016/j.geodrs.2024.e00884.

Clemens, S., Ma, J.F., 2016. Toxic heavy metal and metalloid accumulation in crop plants and foods. Annu. Rev. Plant Biol. 67, 489–512. https://doi.org/10.1146/annurev-arplant-043015-112301.

Cui, F., Xu, X., Wang, M., Ma, S., Lan, C., Fan, P., Cai, Z., 2025. The spatial heterogeneity of soil physical and chemical properties and comprehensive fertility in the Leizhou Peninsula coasta. Sci. Rep. 15, 37178. https://doi.org/10.1038/s41598-025-24112-6.

Custodio, M., Fow, A., Chanamé, F., Orellana-Mendoza, E., Peñaloza, R., Alvarado, J.C., Cano, D., Pizarro, S., 2021. Ecological risk due to heavy metal contamination in sediment and water of natural wetlands with tourist influence in the Central region of Peru. Water (Basel) 13, 2256. https://doi.org/10.3390/w13162256.

Custodio, M., Espinoza, C., Orellana, E., Chanamé, F., Fow, A., Peñaloza, R., 2022. Assessment of toxic metal contamination, distribution and risk in the sediments from lagoons used for fish farming in the Central region of Peru. Toxicol. Rep 9, 1603–1613. https://doi.org/10.1016/j.toxrep.2022.07.016.

Custodio, M., Fow, A., De la Cruz, H., Chanamé, F., Huarcaya, J., 2024. Potential ecological risk from heavy metals in surface sediment of lotic systems in Central region Peru. Front. Water 5. https://doi.org/10.3389/frwa.2023.1295712.

Custodio, M., Pizarro, S., Huarcaya, J., Ortega, K., Ccopi, D., 2025. Ecological and human health risk assessment of heavy metals in mining-affected river sediments in the Peruvian Central Highlands. Toxics 13, 783. https://doi.org/10.3390/toxics13090783.

Dari, B., Rogers, C.W., Leytem, A.B., Schroeder, K.L., 2019. Evaluation of soil test phosphorus extractants in Idaho soils. Soil Sci. Soc. Am. J. 83, 817–824. https://doi.org/10.2136/sssaj2018.08.0314.

Das, R.C., Parvej, S.M.S., Alim, S.M.A., Roy, B.S., Roy, S., 2021. Assessment of heavy metals contamination in road side soils along mymensingh to Valuka Highway. Bangladesh J. Environ. Sci. 40, 122–127.

Davis, N.N., Badger, J., Hahmann, A.N., Hansen, B.O., Mortensen, N.G., Kelly, M., Larsén, X.G., Olsen, B.T., Floors, R., Lizcano, G., et al., 2023. The Global wind Atlas: a high-resolution dataset of climatologies and associated web-based application. Bull. Am. Meteorol. Soc. 104, E1507. https://doi.org/10.1175/BAMS-D-21-0075.1.–E1525.

Ding, Q., Cheng, G., Wang, Y., Zhuang, D., 2017. Effects of natural factors on the spatial distribution of heavy metals in soils surrounding mining regions. Sci. Total Environ. 578, 577–585. https://doi.org/10.1016/j.scitotenv.2016.11.001.

Fick, S.E., Hijmans, R.J., 2017. WorldClim 2: new 1-km spatial resolution climate surfaces for global land areas. Int. J. Climatol. 37, 4302–4315. https://doi.org/10.1002/joc.5086.

Hakanson, L., 1980. An ecological risk index for aquatic pollution control. A sedimentological approach. Water Res. 14, 975–1001. https://doi.org/10.1016/0043-1354(80)90143-8.

Han, J., Mammadov, Z., Mammadov, E., Lee, S., Park, J., Mammadov, G., Elovsat, G., Ro, H.-M., 2019. Elemental composition, leachability assessment and spatial variability analysis of surface soils in the Mugan Plain in the Republic of Azerbaijan,. https://doi.org/10.5194/soil-2019-66.

Haque, F.U., Faridullah, F., Irshad, M., Bacha, A.-U.-R., Ullah, Z., Fawad, M., Hafeez, F., Iqbal, A., Nazir, R., Alrefaei, A.F., et al., 2023. Distribution and speciation of trace elements in soils of four land-use systems. Land (Basel) 12, 1894. https://doi.org/10.3390/land12101894.

Hasi, S.A., Jyoti, S.A., Joardar, J.C., Halder, M., 2025. Heavy metals in the soil, water, plants, and river sediments of Bangladesh: a synthesis. Waste Manag. Bull. 3, 100266. https://doi.org/10.1016/j.wmb.2025.100266.

Hernández-Mendoza, H., Mejuto, M., Cardona, A.I., García-Álvarez, A., Millán, R., Yllera, A., 2013. Optimization and validation of a method for heavy metals quantification in soil samples by inductively coupled plasma sector field mass spectrometry (ICP-SFMS). Am. J. Anal. Chem. 04, 9–15. https://doi.org/10.4236/ajac.2013.410A2002.

Hou, D., Jia, X., Wang, L., McGrath, S.P., Zhu, Y.-G., Hu, Q., Zhao, F.-J., Bank, M.S., O'Connor, D., Nriagu, J., 2025. Global soil pollution by toxic metals threatens agriculture and Human health. Science (1979) 388, 316–321. https://doi.org/10.1126/science.adr5214.

Jia, L., Liang, H., Fan, M., Guo, S., Yue, T., Wang, M., Su, M., Chen, S., Wang, Z., Fu, K., 2024. Spatial distribution and source apportionment of soil heavy metals in the areas affected by non-ferrous metal slag field in Southwest China. Front. Environ. Sci. 12. https://doi.org/10.3389/fenvs.2024.1407319.

Jolliffe, I.T., Cadima, J., 2016. Principal component analysis: a review and recent developments. Philos. Trans. R. Soc. A: Math. Phys. Eng. Sci. 374, 20150202. https://doi.org/10.1098/rsta.2015.0202.

Kolde, R. Pheatmap: pretty heatmaps. CRAN: Contributed Packages 2010.

Lê, S., Josse, J., Rennes, A., Husson, F., 2008. FactoMineR: an R package for multivariate analysis. J. Statist. Soft. 25, 1–18. https://doi.org/10.18637/jss.v025.i01.

Li, Y., Xu, Z., Ren, H., Wang, D., Wang, J., Wu, Z., Cai, P., 2022. Spatial distribution and source apportionment of heavy metals in the topsoil of Weifang City, East China. Front. Environ. Sci. 10. https://doi.org/10.3389/fenvs.2022.893938.

Li, J., Liu, Y., Yang, X., Lu, M., Song, Y., 2026. Spatial variability of soil geochemical elements using a novel ecological factor-incorporated interpretable machine learning model in China's Coastal Saline-Alkali Farmlands. Mar. Pollut. Bull. 222, 118628. https://doi.org/10.1016/j.marpolbul.2025.118628.

Llanos X. AcATaMa – accuracy assessment of thematic maps [QGIS Plugin]. 2024.

Lopez, S.M.E.; Camacho, C.C.A. *Evaluación de La Calidad Del Agua Para El Uso de Riego Agrícola En La Cuenca Del Rio Chancay – Huaral,* 2022; 2022.

Magnani, A., Ajmone-Marsan, F., D'Amico, M., Balestrini, R., Viviano, G., Salerno, F., Freppaz, M., 2018. Soil properties and trace elements distribution along an altitudinal gradient on the southern slope of Mt. Everest, Nepal. Catena (Amst) 162, 61–71. https://doi.org/10.1016/j.catena.2017.11.015.

Mangral, Z.A., Islam, S.U., Tariq, L., Kaur, S., Ahmad, R., Malik, A.H., Goel, S., Baishya, R., Barik, S.K., Dar, T.U.H., 2023. Altitudinal gradient drives significant changes in soil physico-chemical and eco-physiological properties of Rhododendron anthopogon: a case study from Himalaya. Front. For. Glob. Change 6. https://doi.org/10.3389/ffgc.2023.1181299.

edición Traducido adaptado al castellano por Ronald Vargas Rojas Proyecto FAO-SWALIM, C.; Mayor de San Simón, K.-U. *Guía Para La Descripción de Suelos*; 2009.
MINAM Guía Para Muestreo de Suelos 2014, 38.
Minnikova, T., Kolesnikov, S., Sherstnev, A., 2025. Assessment of health of soil in different climatic zones of European part of Russia depending on elemental composition. Soil Secur. 21, 100202. https://doi.org/10.1016/j.soisec.2025.100202.
Montagne, D., Cornu, S., Bourennane, H., Baize, D., Ratié, C., King, D., 2007. Effect of agricultural practices on trace-element distribution in soil. Commun. Soil Sci. Plant Anal. 38, 473–491. https://doi.org/10.1080/00103620601174411.
Muñoz, M.A., Faz, A., Acosta, J.A., Martínez-Martínez, S., Arocena, J.M., 2013. Metal content and environmental risk assessment around high-altitude mine sites. Environ. Earth Sci. 69, 141–149. https://doi.org/10.1007/s12665-012-1942-2.
Muller, G., 1969. Index of geoaccumulation in sediments of the Rhine River. GeoJournal.
Nyengere, J., Okamoto, Y., Funakawa, S., Shinjo, H., 2023. Analysis of spatial heterogeneity of soil physicochemical properties in Northern Malawi. Geoderma Reg. 35, e00733. https://doi.org/10.1016/j.geodrs.2023.e00733.
Omwene, P.I., Öncel, M.S., Çelen, M., Kobya, M., 2018. Heavy metal pollution and spatial distribution in surface sediments of Mustafakemalpaşa Stream located in the World's largest borate basin (Turkey). Chemosphere 208, 782–792. https://doi.org/10.1016/j.chemosphere.2018.06.031.
Öncü, T., Yazman, M.M., Ustaoğlu, F., Hristova, E., Yüksel, B., 2025. Source dynamics and environmental risk of street dust as a vector of Human exposure to potentially toxic elements in Istanbul, Türkiye. Sci. Rep. 15, 30550. https://doi.org/10.1038/s41598-025-11472-2.
Paranavithana, T.M., Mohamed Anas, M.U., Karunaratne, S.B., Macdonald, B., Wimalathunge, N., Bishop, T.F.A., Ratnayake, R.R., 2023. Environmental factors and spatial dependence explain half of the inherent variation in carbon pools of tropical paddy soils. Catena (Amst) 231, 107278. https://doi.org/10.1016/j.catena.2023.107278.
Paun, N., Zgavarogea, R., Niculescu, V.-C., Nasture, A.M., Voicea, I., Popescu (Stegarus), D.I., 2025. From soil to plate: lithium and other trace metals uptake in vegetables under variable soil conditions. Toxics 13, 956. https://doi.org/10.3390/toxics13110956.
Peng, Z., Liang, C., Gao, M., Qiu, Y., Pan, Y., Gao, H., Liu, Y., Li, X., Wei, G., Jiao, S., 2022. The neglected role of micronutrients in predicting soil microbial structure. npj Biofilms Microbiomes 8, 103. https://doi.org/10.1038/s41522-022-00363-3.
Pučko, E., Žibret, G., Teran, K., 2024. Comparison of elemental composition of surface and subsurface soils on national level and identification of potential natural and anthropogenic processes influencing its composition. J. Geochem. Explor. 258, 107422. https://doi.org/10.1016/j.gexplo.2024.107422.
QGIS Development Team QGIS Development Team, 2024. QGIS Geographic Information System (Versión 3.36). Open Source Geospatial Foundation.
Qi, C., Hu, T., Zheng, Y., Wu, M., Tang, F.H.M., Liu, M., Zhang, B., Derrible, S., Chen, Q., Hu, G., et al., 2025. Global and regional patterns of soil metal(Loid) mobility and associated risks. Nat. Commun. 16, 2947. https://doi.org/10.1038/s41467-025-58026-8.
R Core Team, 2024. R: A Language and Environment for Statistical Computing. R Foundation for Statistical Computing, Vienna, Austria. https://www.R-project.org/.
Rahayu, R., Supriyadi, S., Herdiansyah, G., Herawati, A., Erdaswin, F., 2023. The influence of geological formations on soil characteristics and quality in the Southeast Region of Pacitan Regency, Indonesia. Soil Sci. Annu. 74, 1–13. https://doi.org/10.37501/soilsa/175383.
Rate, A.W., 2021. Spatial analysis of soil trace element contaminants in urban public open space, Perth, Western Australia. Soil Syst. 5, 46. https://doi.org/10.3390/soilsystems5030046.
Ritz, K., McNicol, J.W., Nunan, N., Grayston, S., Millard, P., Atkinson, D., Gollotte, A., Habeshaw, D., Boag, B., Clegg, C.D., et al., 2004. Spatial structure in soil chemical and microbiological properties in an upland grassland. FEMS Microbiol. Ecol. 49, 191–205. https://doi.org/10.1016/j.femsec.2004.03.005.
Rivera, H.; Chira, J.; Chacón, Í.; Medina, A.; Casallo, I. *Geodisponibilidad de Metales Pesados en sedimentos de Los Ríos Supe y Pativilca, Departamento de Lima Geo-availability of heavy metals in sediments of Supe and Pativilca River, Lima Department*; 2011; Vol. 14;.
Rosas, M.A., Viveen, W., Vanacker, V., 2023. Spatial variation in specific sediment yield along the Peruvian western Andes. Catena (Amst) 220, 106699. https://doi.org/10.1016/j.catena.2022.106699.
Santos-Francés, F., Martínez-Graña, A., Zarza, C., Sánchez, A., Rojo, P., 2017. Spatial distribution of heavy metals and the environmental quality of soil in the Northern plateau of Spain by geostatistical methods. Int. J. Environ. Res. Public Health 14, 568. https://doi.org/10.3390/ijerph14060568.
Schneider, H.M., Ben-Gal, A., Furtado, B., Cicek, N., Dalmaris, E., Atzori, G., Bazihizina, N., 2026. Going underground: the importance of soil heterogeneity in shaping plant productivity and responses to saline soils. Environ. Exp. Bot. 243, 106321. https://doi.org/10.1016/j.envexpbot.2026.106321.
Shao, Y., Ma, W., Chen, Y., Lv, Y., Wang, N., Lin, J., Lv, Y., Li, H., 2026. Variations in source-originated health risks of soil heavy metals in an open-pit mining area, Northern China from 2014 to 2023. J. Environ. Sci. https://doi.org/10.1016/j.jes.2026.01.049.
Song, H., Hu, K., An, Y., Chen, C., Li, G., 2018. Spatial distribution and source apportionment of the heavy metals in the agricultural soil in a regional scale. J. Soils Sediments 18, 852–862. https://doi.org/10.1007/s11368-017-1795-0.
Sun, C., Liu, J., Wang, Y., Sun, L., Yu, H., 2013. Multivariate and geostatistical analyses of the spatial distribution and sources of heavy metals in agricultural soil in Dehui, Northeast China. Chemosphere 92, 517–523. https://doi.org/10.1016/j.chemosphere.2013.02.063.
Sun, J., Li, H., JianJi, G., He, Y., Xu, L., Zhang, L., Guan, Q., Ye, Y., Xu, C., Wang, H., 2025. Influence of altitudinal zones on soil nutrient dynamics and fertility constraints in agricultural terrains of Yunnan, China. Sci. Rep. 15, 43452. https://doi.org/10.1038/s41598-025-27297-y.
Tang, H., Deng, Q., Yuan, Y., Zhang, S., Luo, Y., Chen, Y., Jiang, L., Huang, Y., 2024. The spatial distribution and source of heavy metals in soil-plant-atmosphere system in a large coal mining area. Ore Energy Resour. Geol. 17, 100059. https://doi.org/10.1016/j.oreoa.2024.100059.
Taylor, S.R., Mclennan, S.M., 1995. The geochemical the Continental evolution crust. Rev. Miner. Geochem. 33, 241–265.
Tokatlı, C., Ustaoğlu, F., Yazman, M.M., Yüksel, B., 2026. Where rivers meet the sea: source fingerprinting and health risk mapping of potentially hazardous elements in sediments from the Çanakkale Strait Basin (Türkiye). Mar. Pollut. Bull. 222, 118626. https://doi.org/10.1016/j.marpolbul.2025.118626.
Turekian, K.K., Wedepohl, K.H., Karl, K., 1961. TUREKIAN Dept. Geology, Yale University, New Haven, Conn. KARL HANS WEDEPOHL Mineralogische-Institut Der Universitat, Gottingen, Germany distribution of the elements in some major units of the Earth's crust. America (NY) 175–192.
U.S. EPA., 2007. Method 3051A (SW-846): Microwave Assisted Acid Digestion of Sediments, Sludges, Soils, and Oils. Revision 1. Washington, DC. Available online: (accessed 27 February 2026), https://www.epa.gov/esam/us-epa-method-3051a-microwave-assisted-acid-digestion-sediments-sludges-and-oils.
U.S. EPA. *Method 6020B (SW-846): inductively coupled plasma-mass spectrometry*; Washington, DC, 2014.
Vargas, R.L.; De La Cruz, P.C.; Pascual, G.O.; Aguilar, J.P.; Agurto, C.A.; Vargas, G.J.; Trelles Vásquez, G.; Espinoza, V.I.; Amado, R.J.; Chero, I.D. *Geoquimica Multipropósito de Suelos En Las Zona Jauja–Acostambo*; INGEMMET: Lima, Peru, 2022. Available online: https://repositorio.ingemmet.gob.pe/handle/20.500.12544/3595 (accessed 11 May 2026).
Velazco, J., Pinilla, V., 2018. Development models, agricultural policies and agricultural growth: Peru, 1950–2010. Agricultural Development in the World Periphery. Springer International Publishing, Cham, pp. 413–438.
Venkateswarlu, M., Rallapalli, S., Singh, A., Chalapathi, G.S.S., Kumar, S., Katpatal, Y.B., Sujatha, G., 2025. Macro and micronutrient based soil fertility zonation using fuzzy logic and geospatial techniques. Sci. Rep. 15, 26772. https://doi.org/10.1038/s41598-025-12184-3.
Vereecken, H., Schnepf, A., Hopmans, J.W., Javaux, M., Or, D., Roose, T., Vanderborght, J., Young, M.H., Amelung, W., Aitkenhead, M., et al., 2016. Modeling soil processes: review, key challenges, and new perspectives. Vadose Zone J. 15, 1–57. https://doi.org/10.2136/vzj2015.09.0131.
Villalobos Segura, I.C., Melquiades Valles, J.L., Neyra Ramos, F.-I., Ramos Avila, D.A., Vega-Gonzalez, J.A., Cotrina Teatino, M.A., Portilla Rodriguez, H.R., 2023. Exploration, development and exploitation of mining and metallurgical minerals in Peru. In: Proceedings of the Exploración, desarrollo y explotación minero metalúrgico del Perú; Latin American and Caribbean Consortium of Engineering Institutions.
Walter, M.; De Piérola, J.C.; Cooper, C.; Zegarra, D.; Diez Canseco, C.; Gobitz, V.; Laguna, R.; Liendo, C. *Minería en Perú 2021-2030: ¿qué Rol Juega en La Reactivación Económica y El Desarrollo Territorial?: Estudio y Recomendaciones Sectoriales*; Washington, D. C., 2021.
Wei, T., Simko, V., 2010. Corrplot: visualization of a correlation matrix. CRAN: contributed packages.
Wickham, H., François, R., Henry, L., Müller, K., Vaughan, D., 2014. Dplyr: a grammar of data manipulation. CRAN: Contributed Packages.
Wickham, H., Averick, M., Bryan, J., Chang, W., McGowan, L., François, R., Grolemund, G., Hayes, A., Henry, L., Hester, J., et al., 2019. Welcome to the Tidyverse. J. Open Source Softw. 4, 1686. https://doi.org/10.21105/joss.01686.
Wickham, H., 2016. Ggplot2. Springer International Publishing, Cham. ISBN 978-3-319-24275-0.
Wilson, M.J., 2019. The importance of parent material in soil classification: a review in a historical context. Catena (Amst) 182, 104131. https://doi.org/10.1016/j.catena.2019.104131.
Wu, W., Li, Y., Yan, M., Yang, L., Lei, J., Liu, H.-B., 2021. Surface soil metal elements variability affected by environmental and soil properties. PLoS One 16, e0254928. https://doi.org/10.1371/journal.pone.0254928.
Wu, Y., Zhou, L., Meng, Y., Lin, Q., Fei, Y., 2023. Influential topographic factor identification of soil heavy metals using GeoDetector: the effects of DEM resolution and pollution sources. Remote Sens. (Basel) 15, 4067. https://doi.org/10.3390/rs15164067.
Xing, Y., Xie, Y., Wang, X., 2025. Enhancing soil health through balanced fertilization: a pathway to sustainable agriculture and food security. Front. Microbiol. 16. https://doi.org/10.3389/fmicb.2025.1536524.
Yüksel, B., Ustaoğlu, F., 2025. Pollution analysis of metals in the sediments of lagoon lakes in Türkiye: toxicological risk assessment and source insights. Process Saf. Environ. Prot. 193, 665–682. https://doi.org/10.1016/j.psep.2024.11.085.
Yüksel, B., Öncü, T., Yazman, M.M., Hristova, E., Ustaoglu, F., 2025. P30-07 Assessment of potentially toxic elements in urban street dust of Istanbul: spatial distribution, source apportionment, and health risk implications. Toxicol. Lett. 411, S377. https://doi.org/10.1016/j.toxlet.2025.07.870. –S377a.
Yavitt, J.B., Harms, K.E., Garcia, M.N., Wright, S.J., He, F., Mirabello, M.J., 2009. Spatial heterogeneity of soil chemical properties in a lowland tropical moist forest, Panama. Soil Res. 47, 674–687. https://doi.org/10.1071/SR08258.
Zanaga, D.; Ruben Daems; Dirk De Keersmaecker; Wanda Brockmann; Carsten Kirches; Grit Wevers; Jan Cartus; Oliver Santoro; Maurizio Fritz; Steffen Lesiv; et al. ESA WorldCover 10 m 2020 V100 2021.

Zeng, J., Tan, L., Guo, Z., Wang, J., Wei, Y., Cai, C., 2026. Spatial heterogeneity of soil functions in the gully vicinity within a watershed: coupling effects of landscape characteristics and ridge practices. Catena (Amst) 265, 109866. https://doi.org/10.1016/j.catena.2026.109866.

Zhang, Q., Han, G., Liu, M., Liang, T., 2019. Spatial distribution and controlling factors of heavy metals in soils from Puding Karst Critical Zone Observatory, Southwest China. Environ. Earth Sci. 78, 279. https://doi.org/10.1007/s12665-019-8280-6.

Zhang, H., Zeng, H., Jiang, Y., Xie, Z., Xu, X., Ding, M., Wang, P., 2020. Using the compound system to synthetically evaluate the enrichment of heavy metal(Loid)s in a subtropical basin, China. Environ. Pollut. 256, 113396. https://doi.org/10.1016/j.envpol.2019.113396.

Zhang, Q., Liu, H., Mei, X., Gu, Z., Li, X., 2025. Topography-driven variability in atmospheric deposition and soil distribution of cadmium, lead and zinc in a mountainous agricultural area. Sci. Rep. 15, 20894. https://doi.org/10.1038/s41598-025-05258-9.

Zhou, H., Yan, Y., Dai, Q., He, Z., Yi, X., 2023. Latitudinal and altitudinal patterns and influencing factors of soil humus carbon in the low-latitude plateau regions. Forests 14, 344. https://doi.org/10.3390/f14020344.